

several genes remained unaffected by the extra rapid cell cycles (fig. S8A), underlining that several mechanisms regulate mRNA abundance at the MBT (*I*).

To understand the physiological importance of the regulation of DNA replication during development, we analyzed the phenotype of embryos overexpressing RecQ4, Treslin, Drf1, and Cut5. Embryos that overexpress these four factors failed to complete gastrulation and blastopore closure at stage 10.5 (Fig. 4) and underwent cell death by stage 17 (neurula), showing that titration of these factors is critical for embryogenesis.

If this developmental defect upon overexpression of RecQ4, Treslin, Drf1, and Cut5 is indeed due to increased rates of initiation, we hypothesized that a partial reduction in origin licensing might suppress this phenotype. Injection of embryos with morpholinos against the pre-RC component *cdc6* resulted in partial depletion of the Cdc6 protein (Fig. 4, top), and although this caused a slight delay in blastopore closure, 81% of these morpholino-injected embryos reached the neurula stage (Fig. 4). However, coinjection of these *cdc6* morpholinos together with overexpression of RecQ4, Treslin, Drf1, and Cut5 partially rescued the ability of these embryos to undergo gastrulation, and 38% of embryos survived until stage 17. This indicates that the developmental deficiency caused by overexpression of RecQ4, Treslin, Drf1, and Cut5 is at least in part due to the resulting increase in replication initiation. The *cdc6* morpholinos in combination with the overexpression of limiting initiation factors not only partially rescued the embryonic defect but also restored normal cell cycle elongation and Chk1 activation at the MBT (fig. S9). Together, these experiments

demonstrate that the regulation of replication initiation rates is necessary for several of the critical events of the MBT and for normal development in *Xenopus laevis*.

This study provides a mechanistic basis for the hypothesis put forward 30 years ago that passive depletion of limiting factors by the N/C ratio is the primary mechanism controlling events at the MBT (*4*). We speculate that the interplay between the limiting replication factors RecQ4, Treslin, Drf1, and Cut5, together with Chk1 activation and CDK inactivation, forms a feedback loop (fig. S10), which in accordance with work in flies (*3, 6, 25, 26*) underlies how *S*-phase length is regulated during development across eukaryotes.

References and Notes

1. W. Tadros, H. D. Lipshitz, *Development* **136**, 3033–3042 (2009).
2. K. Shimuta *et al.*, *EMBO J.* **21**, 3694–3703 (2002).
3. O. C. Sibon, V. A. Stevenson, W. E. Theurkauf, *Nature* **388**, 93–97 (1997).
4. J. Newport, M. Kirschner, *Cell* **30**, 675–686 (1982).
5. J. Newport, M. Kirschner, *Cell* **30**, 687–696 (1982).
6. P. Fogarty *et al.*, *Curr. Biol.* **7**, 418–426 (1997).
7. O. Hyrien, C. Maric, M. Méchali, *Science* **270**, 994–997 (1995).
8. S. L. McKnight, O. L. Miller Jr., *Cell* **12**, 795–804 (1977).
9. A. B. Blumenthal, H. J. Kriegstein, D. S. Hogness, *Cold Spring Harb. Symp. Quant. Biol.* **38**, 205–223 (1974).
10. T. S. Takahashi, J. C. Walter, *Genes Dev.* **19**, 2295–2300 (2005).
11. T. Silva, R. H. Bradley, Y. Gao, M. Coue, *J. Biol. Chem.* **281**, 11569–11576 (2006).
12. A. Kumagai, A. Shevchenko, A. Shevchenko, W. G. Dunphy, *J. Cell Biol.* **193**, 995–1007 (2011).
13. K. Matsuno, M. Kumano, Y. Kubota, Y. Hashimoto, H. Takisawa, *Mol. Cell. Biol.* **26**, 4843–4852 (2006).
14. M. N. Sangrithi *et al.*, *Cell* **121**, 887–898 (2005).

15. J. Walter, J. W. Newport, *Science* **275**, 993–995 (1997).
16. B. A. Edgar, C. P. Kiehle, G. Schubiger, *Cell* **44**, 365–372 (1986).
17. J. Newport, M. Dasso, *J. Cell Sci. Suppl.* **1989** (suppl. 12), 149–160 (1989).
18. J. A. Howe, J. W. Newport, *Proc. Natl. Acad. Sci. U.S.A.* **93**, 2060–2064 (1996).
19. R. S. Hartley, J. C. Sible, A. L. Lewellyn, J. L. Maller, *Dev. Biol.* **188**, 312–321 (1997).
20. D. Mantiero, A. Mackenzie, A. Donaldson, P. Zegerman, *EMBO J.* **30**, 4805–4814 (2011).
21. L. Vastag *et al.*, *PLoS ONE* **6**, e16881 (2011).
22. H. R. Woodland, R. Q. Pestell, *Biochem. J.* **127**, 597–605 (1972).
23. D. Kimelman, M. Kirschner, T. Scherson, *Cell* **48**, 399–407 (1987).
24. X. Lu, J. M. Li, O. Elemento, S. Tavazoie, E. F. Wieschaus, *Development* **136**, 2101–2110 (2009).
25. A. W. Shermoen, M. L. McClelland, P. H. O'Farrell, *Curr. Biol.* **20**, 2067–2077 (2010).
26. M. L. McClelland, A. W. Shermoen, P. H. O'Farrell, *J. Cell Biol.* **187**, 7–14 (2009).

Acknowledgments: We are grateful to T. Takahashi, J. Walter, V. Costanzo, J. Diffley, H. Takisawa, and R. Laskey for reagents. DNA combing analysis was performed with assistance from V. Gaggioli. We are grateful to J. Pines, R. Laskey, and members of the Zegerman group for critical reading of this manuscript and S. Di Talia for discussions. P.Z. is funded by AICR 10-0908. J.C.S. and C.C. were supported by the Wellcome Trust and by the UK Medical Research Council (programme no. U117597140). All authors acknowledge the core support provided by CRUK C6946/A14492 and the Wellcome Trust 092096.

Supplementary Materials

www.sciencemag.org/cgi/content/full/science.1241530/DC1
Materials and Methods
Figs. S1 to S10
Movie S1
Reference (27)

5 June 2013; accepted 23 July 2013
Published online 1 August 2013;
10.1126/science.1241530

SGK196 Is a Glycosylation-Specific O-Mannose Kinase Required for Dystroglycan Function

Takako Yoshida-Moriguchi,¹ Tobias Willer,¹ Mary E. Anderson,¹ David Venzke,¹ Tamiaka Whyte,² Francesco Muntoni,² Hane Lee,³ Stanley F. Nelson,³ Liping Yu,⁴ Kevin P. Campbell^{1*}

Phosphorylated *O*-mannosyl trisaccharide [*N*-acetylgalactosamine- β 3-*N*-acetylglucosamine- β 4-(phosphate-6)-mannose] is required for dystroglycan to bind laminin-G domain-containing extracellular proteins with high affinity in muscle and brain. However, the enzymes that produce this structure have not been fully elucidated. We found that glycosyltransferase-like domain-containing 2 (GTDC2) is a protein *O*-linked mannosyl β 1,4-*N*-acetylglucosaminyltransferase whose product could be extended by β 1,3-*N*-acetylgalactosaminyltransferase2 (B3GALNT2) to form the *O*-mannosyl trisaccharide. Furthermore, we identified SGK196 as an atypical kinase that phosphorylated the 6-position of *O*-mannose, specifically after the mannosyl had been modified by both GTDC2 and B3GALNT2. These findings suggest how mutations in GTDC2, B3GALNT2, and SGK196 disrupt dystroglycan receptor function and lead to congenital muscular dystrophy.

Posttranslational modification of proteins via stringently regulated biosynthetic pathways extends their range of function. Defects in the posttranslational modification of the

dystroglycan (DG) protein are common to a variety of congenital muscular dystrophies (CMDs)—including Walker-Warburg syndrome (WWS), Fukuyama CMD, muscle-eye-brain disease, and

certain types of limb-girdle muscular dystrophy—and result in the malfunction of DG as an extracellular matrix (ECM) receptor (*1*). DG is composed of a transmembrane β subunit and a cell-surface α subunit (*2*). α -DG serves as a receptor for laminin-G domain-containing ECM ligands, including laminin, perlecan, agrin, and neurexin (*2*), which involves various types of glycosylation of its mucin domain. In particular, phosphorylation at the 6-position of an *O*-mannose of the trisaccharide [*N*-acetylgalactosamine (GalNAc)- β 3-*N*-acetylglucosamine (GlcNAc)- β 4-mannose]

¹Howard Hughes Medical Institute, Department of Molecular Physiology and Biophysics, Department of Neurology, Department of Internal Medicine, University of Iowa Roy J. and Lucille A. Carver College of Medicine, 4283 Carver Biomedical Research Building, 285 Newton Road, Iowa City, IA 52242–1101, USA. ²Dubowitz Neuromuscular Centre, Division of Neuroscience, Institute of Child Health and Great Ormond Street Hospital for Children, London, UK. ³Department of Human Genetics, David Geffen School of Medicine, University of California, Los Angeles, CA 90095, USA. ⁴Medical Nuclear Magnetic Resonance Facility, University of Iowa Roy J. and Lucille A. Carver College of Medicine, B291 Carver Biomedical Research Building, 285 Newton Road, Iowa City, IA 52242–1101, USA.

*Corresponding author. E-mail: kevin-campbell@uiowa.edu

produces a branch chain that is ultimately extended with repeating disaccharides [α -3-glucuronic acid (GlcA) β -3-xylose (Xyl)] synthesized by like-acetylglucosaminyltransferase (LARGE), enabling α -DG to bind ECM ligands (3, 4). Mutations in several known and putative glycosyltransferases cause DG-related disorders. Recently, genetic studies of the DG-related diseases CMD and cobblestone lissencephaly identified several new causative genes, including *isoprenoid synthase domain containing* (*ISPD*) (5), *transmembrane protein 5* (*TMEM5*) (6), β 1,3-*N*-acetylglucosaminyltransferase (*B3GNT1*) (7), *glycosyltransferase-like domain containing 2*

(*GTDC2*) (8), β 3-*N*-acetylgalactosaminyltransferase2 (*B3GALNT2*) (9), and *SGK196* (10). However, the functions of the genes' products remain largely unknown.

O-Mannosyl glycosylation of α -DG is initiated by the endoplasmic reticulum (ER)-resident protein *O*-mannosyl transferase 1/2 complex (*POMT1/2*), which adds mannose to Ser/Thr residues (11). To help to clarify the functions of the recently identified causative proteins, we examined their sub-cellular localization. *GTDC2* was present in the ER (Fig. 1A), suggesting that it might modify the above-described *O*-mannose. Thus, we synthesized

a peptide corresponding to the mucinlike domain of human α -DG (residues 316 to 329), in which Thr³¹⁷ was modified by *O*-mannose but the remaining Thr/Ser residues were replaced with Ala. The glycopeptide was incubated with c-Myc-tagged *GTDC2* (*GTDC2*-Myc) purified from human embryonic kidney (HEK) 293 cell lysates, as well as various nucleotide sugars. Matrix-assisted laser desorption-ionization time-of-flight mass spectrometry (MALDI-TOF/MS) analysis suggested that *GTDC2*-Myc transferred *N*-acetylhexosamine to the glycopeptide (fig. S1). Repetition of this assay using uridine 5'-diphosphate (UDP)-GlcNAc

Fig. 1. *GTDC2* has a protein *O*-linked mannose β 1,4-*N*-acetylglucosaminyltransferase activity.

(A) HEK293 cells expressing c-Myc-tagged *GTDC2* were stained with anti-Myc (green), ERp72 (ER marker, red), and 4',6-diamidino-2-phenylindole (DAPI, nuclei, blue). Scale bars indicate 10 μ m. (B) The product of the *GTDC2* in vitro assay when a DG-derived peptide modified with *O*-linked mannose and UDP-GlcNAc were used as substrates was analyzed by MALDI-TOF/MS. A, Ala; G, Gly; H, His; I, Ile; P, Pro; T, Thr; V, Val. a.u., arbitrary units; *m/z*, mass to charge ratio. (C) Reactant of the *GTDC2*dTM assay using Man α -MU and UDP-GlcNAc was separated on Superdex Peptide 10/300 (GE Healthcare) columns. S, unreacted acceptor substrate. P, enzymatic product. (D) Structure of the product in (C), with the sugar subunits labeled A and B. HMQC (E) and overlay (F) of the HMQC (black and red) and HMBC (green) spectra of the product. Assigned cross-peaks are labeled with a first letter representing the subunit [as designated in (D)], and the rest of the label represents the position on that subunit. The red peak in (E) is the folded peak. ppm, parts per million.

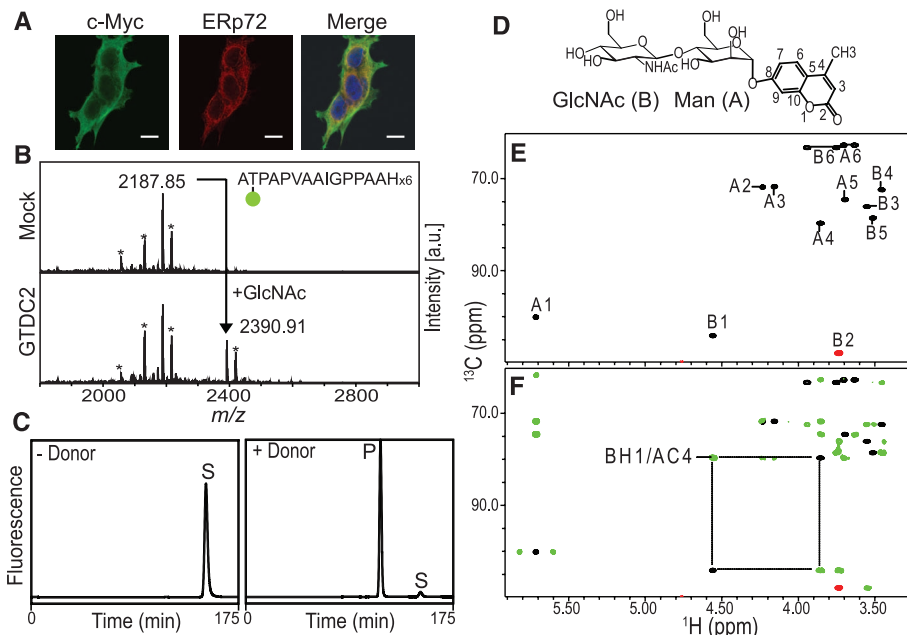


Fig. 2. Mutations in *GTDC2* and *B3GALNT2* cause defects in the synthesis of phosphorylated α -DG.

(A) The product of the *B3GALNT2*dTM in vitro assay using the product depicted in Fig. 1B and UDP-GalNAc as substrates was analyzed by MALDI-TOF/MS. (B) Laminin (open circles, left) and WFA (open circles, right) binding to DG-derived peptide modified with the GalNAc β -3-GlcNAc β -4-mannose was measured by solid-phase assay (*n* = 3). The trisaccharide-modified peptide produced by the *GTDC2*dTM and *B3GALNT2*dTM reactions was conjugated to maleimide-activated plates. The peptide modified with mannose was used for background subtraction. Wild-type muscle glycoproteins (solid circles) served as positive control in the laminin-binding assay. Error bars indicate SD. (C) Fc-tagged DGfc340 was produced in [³²P]-orthophosphate-labeled fibroblasts derived from a control individual and *GTDC2*- or *B3GALNT2*-mutated patients. DGfc340 was isolated from the culture medium by using protein-A agarose, separated by SDS-polyacrylamide gel electrophoresis, stained with Coomassie brilliant blue (CBB), and analyzed by phosphorimaging ([³²P]). Mr, relative molecular mass. (D) Reactants of rabbit brain total membrane fraction incubated with ATP and GalNAc β -3-GlcNAc β -4-Man α -MU at 37°C for 6 hours were separated on a C18 reverse-phase column. S, unreacted acceptor substrate. P, enzymatic product.

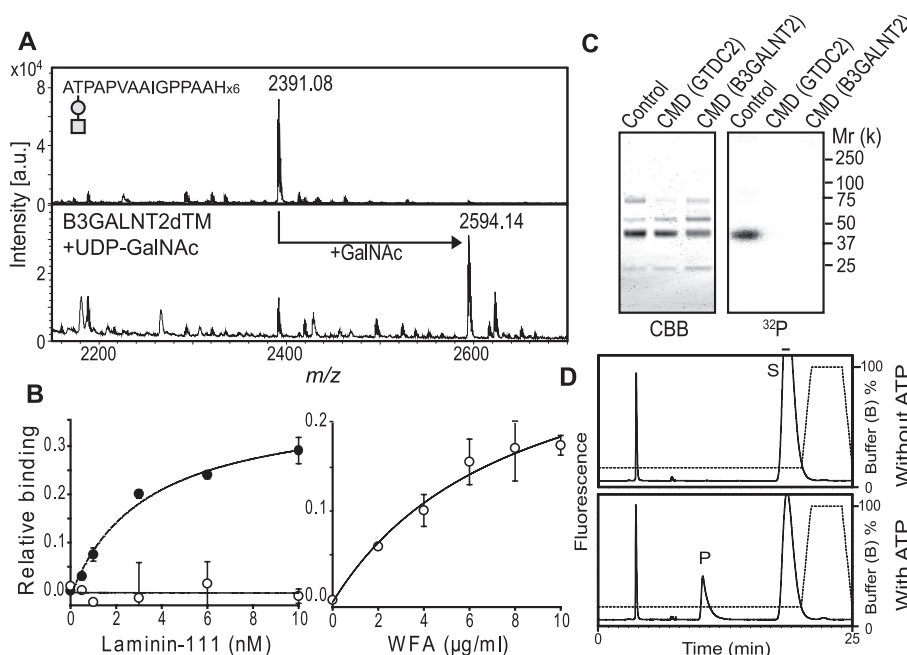
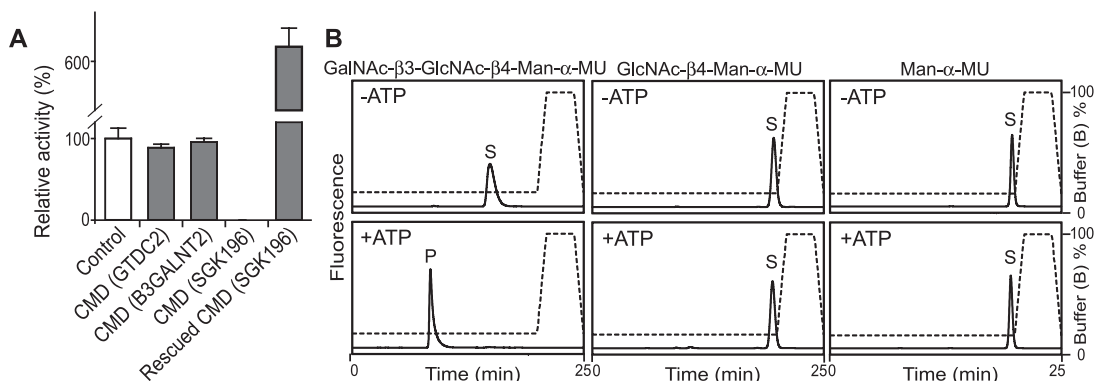


Fig. 3. SGK196 phosphorylates GalNAc-β3-GlcNAc-β4-Man.

(A) Cell lysates from control fibroblasts and fibroblasts derived from patients with a mutation in SGK196, GTDC2, or B3GALNT2, as well as SGK196 patient-derived fibroblasts ectopically expressing SGK196-Myc-DDK, were subjected to a kinase assay using GalNAc-β3-GlcNAc-β4-Man-α-MU. Data obtained from three individual experiments are shown, with error bars indicating SD. (B) Reactants from a phosphorylation assay in which SGK196-Myc-DDK was used were separated on a C18 reverse-phase column. GalNAc-β3-GlcNAc-β4-Man-α-MU (left), GlcNAc-β4-Man-α-MU (middle), or Man-α-MU (right) was used as acceptor in the absence (top) or presence (bottom) of ATP.



(Fig. 1B) or UDP-GalNAc (fig. S2) as the donor confirmed that the transfer was specific to GlcNAc and that it did not occur when GTDC2-Myc carrying a mutation found in a CMD patient was used (fig. S2). Next, we prepared a secreted form of GTDC2 (lacking the transmembrane domain; GTDC2dTM) in HEK293 cells (fig. S3) and conducted the transfer assay by using fluorescently labeled mannoside (4-methylumbelliferyl-α-D-mannoside; Man-α-MU) as the acceptor. The product was purified by gel filtration (Fig. 1C) and then analyzed by nuclear magnetic resonance (NMR). The ¹H and ¹³C resonances of the product were assigned by using heteronuclear multiple quantum coherence (HMQC) and heteronuclear 2-bond correlation (H2BC) spectra (fig. S4; Fig. 1, D and E; table S1). Rotating-frame Overhauser enhancement (ROE) data (fig. S5) confirmed that GlcNAc has a beta configuration. A BH1/AC4 cross-peak detected by the heteronuclear multiple bond correlation (HMBC) spectrum (Fig. 1F) indicated that the GlcNAc was linked to the 4-position of the mannose. Thus, GTDC2 possesses a protein *O*-mannose β1,4-*N*-acetylglucosaminyltransferase activity.

Human B3GALNT2, mutations in which cause WWS (9), has been cloned on the basis of its β3-glycosyltransferase motifs. This enzyme is thought to act as a β1,3-*N*-acetylgalactosaminyltransferase that uses β-linked GlcNAc as its acceptor in vitro (12). However, the GalNAc-β3-GlcNAc-β sequence had not been found in mammals when the gene was cloned, leaving the biological importance of this enzyme unclear. α-DG contains an *O*-mannosyl glycan (GalNAc-β3-GlcNAc-β4-Man), with the mannose phosphorylated at the 6-position (3). The ECM-ligand-binding moiety of α-DG extends from this phosphate residue (3). To test whether B3GALNT2 and GTDC2 act coordinately on *O*-mannose to synthesize this trisaccharide, we prepared a secreted form of B3GALNT2 (B3GALNT2dTM) (fig. S6) and incubated this protein with UDP-GalNAc and the GlcNAc-β4-Man-*O*-peptide produced by the GTDC2dTM reaction. MALDI-TOF/MS analysis confirmed that B3GALNT2 could transfer a GalNAc residue to the acceptor (Fig. 2A), suggesting that

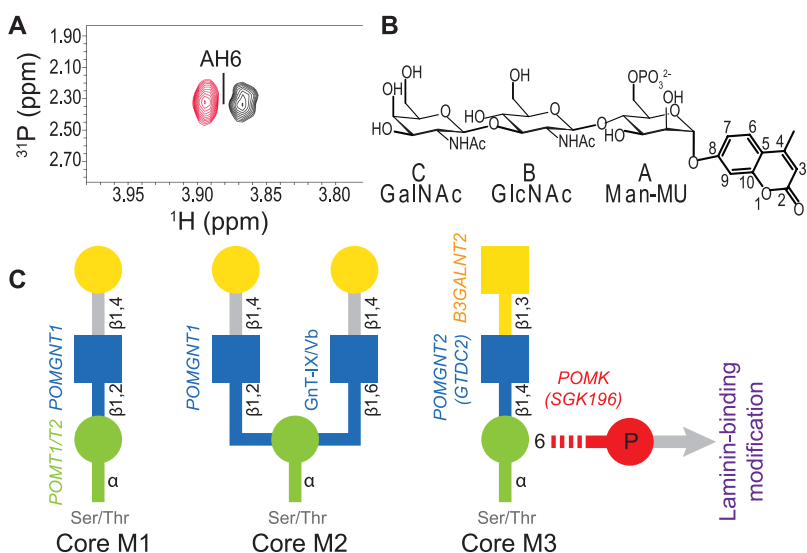


Fig. 4. SGK196 phosphorylates the 6-position of *O*-mannose. (A) The ³¹P/¹H correlation spectroscopy spectrum of the product depicted in Fig. 3B when GalNAc-β3-GlcNAc-β4-Man-α-MU was used as the acceptor. Assigned cross-peaks were labeled as described in Fig. 1 by using the subunit designation indicated in (B). (B) Structure of the phosphorylated product, with sugar subunits labeled A to C. (C) Model of α-DG glycan structures. Proposed classification of each *O*-mannosyl core structure is indicated at bottom. Enzymes responsible for forming the respective linkages are indicated at left; those identified as causing (POMT1/2, POMGNT1 and 2, B3GALNT2, and POMK) DG-related disorders are indicated in italics. Green circle, Man; blue square, GlcNAc; yellow circle, Gal; yellow square, GalNAc; red circle, phosphate.

B3GALNT2 and GTDC2 can synthesize GalNAc-β3-GlcNAc-β4-Man. CMD patients who have mutations in these genes produce α-DG with pathological defects in ECM binding (8, 9). We next used a solid-phase laminin-binding assay to test whether the GalNAc-β3-GlcNAc-β terminus contributes directly to the binding of α-DG to ECM ligands. Whereas the GalNAc-β3-GlcNAc-β4-Man-modified peptide exhibited significant affinity for *Wisteria floribunda* lectin (WFA, which recognizes terminal GalNAc residues), this was not the case for laminin-111 (Fig. 2B). Next we asked whether a defect in synthesis of the GalNAc-β3-GlcNAc-β terminus prevented *O*-mannose from being further modified by phosphorylation. We expressed Fc-tagged recombinant DG (DGFc340), which contains the region in

which the functional modification occurs (13), in [³²P]-orthophosphate-labeled control fibroblasts and CMD patient fibroblasts with mutations in GTDC2 or B3GALNT2 (Fig. 2C). Indeed, the cells from the CMD patients did not produce [³²P]-phosphorylated DGFc340, indicating that phosphorylation of the α-DG *O*-mannose is inhibited by lack of the GalNAc-β3-GlcNAc-β terminus from the mannose.

To understand how the *O*-glycan on α-DG is phosphorylated, we synthesized fluorescently labeled GalNAc-β3-GlcNAc-β4-Man by using GTDC2dTM, B3GALNT2dTM, and the acceptor Man-α-MU. We first tested adenosine triphosphate (ATP) as a phosphate donor, by performing the assay on total membrane fractions obtained from rabbit brain with GalNAc-β3-GlcNAc-β4-Man-α-MU

as the acceptor. Separation of the reactant on a C18 column revealed that GalNAc- β 3-GlcNAc- β 4-Man- α -MU (Fig. 2D) was phosphorylated in the presence of ATP. We further separated the ER and Golgi complex in mouse liver membrane fractions and found that the phosphorylation activity resided in the ER fractions (fig. S7). Causative proteins of DG-related disorders whose functions remain unknown include fukutin (FKTN), fukutin-related protein (FKRP), TMEM5, ISPD, and SGK196. Among these, only SGK196 shares homology with known protein kinases, although it is believed to be inactive because of the high divergence of its putative kinase domains from the consensus sequence (14). We tested its phosphorylation activity in lysates from control fibroblasts and CMD patient fibroblasts with mutations in SGK196, GTDC2, or B3GALNT2. The activity toward GalNAc- β 3-GlcNAc- β 4-Man- α -MU was lacking only in the SGK196-mutated cells, and this loss was rescued by ectopic expression of c-Myc-DDK (FLAG)-tagged SGK196 (SGK196-Myc-DDK) (Fig. 3A). When SGK196-Myc-DDK produced in HEK293 cells was incubated with ATP and/or Man- α -MU derivatives, SGK196 exhibited significant phosphorylation activity toward GalNAc- β 3-GlcNAc- β 4-Man- α -MU. Moreover, this activity was not observed when GlcNAc- β 4-Man- α -MU or Man- α -MU was used as the acceptor (Fig. 3B). Phosphorylated GalNAc- β 3-GlcNAc- β 4-Man- α -MU was not detected when SGK196-Myc-DDK carrying a mutation (Leu¹³⁷→Arg¹³⁷) found in a CMD patient (10) was used in the assay (fig. S8). To elucidate the enzymatic properties of SGK196, we produced a soluble form of SGK196 (SGK196dTM, fig. S9). Its phosphorylation activity depended on divalent ions with an apparent Michaelis constant for ATP of $4.1 \pm 1.4 \mu\text{M}$ (fig. S10). To pinpoint which hydroxyl group of the trisaccharide is phosphorylated by SGK196, we isolated the product obtained in the experiment depicted in Fig. 3B and analyzed its structure by NMR. The ¹H and ¹³C resonances of the product were assigned on the basis of HMQC, HMBC, and H2BC spectra (fig. S11 and table S2), and the anomeric configurations were determined by ROE (fig. S12). The BH1/AC4 and CH1/BC3 cross-peaks detected in the HMBC spectrum confirmed that the GalNAc and GlcNAc residues were attached to GlcNAc and Man via β 1-3 and β 1-4 linkages, respectively (fig. S11). The phosphate group added by SGK196 was attached to the 6-position of the mannose residue (Fig. 4, A and B).

We have shown that GTDC2 has a protein *O*-mannose β 1,4-*N*-acetylglucosaminyltransferase activity, which leads us to designate it as POMGNT2, and that GTDC2 and B3GALNT2 can synthesize a GalNAc- β 3-GlcNAc- β -terminus at the 4-position of protein *O*-mannose. SGK196 phosphorylated the 6-position of *O*-mannose by using ATP, and on this basis we propose to designate it as a protein *O*-mannose kinase (POMK). Because SGK196 lacks certain residues required for catalysis by kinases (14), the mechanism used to

catalyze the phosphotransfer reaction is unclear. SGK196 exhibited the phosphorylation activity only when the GalNAc- β 3-GlcNAc- β -terminus was linked to the 4-position of *O*-mannose, indicating that this disaccharide serves as the substrate recognition motif of SGK196. This strict specificity of SGK196 may explain why mutations in GTDC2 and B3GALNT2 cause DG-related disorders although their product does not directly recognize the ECM ligand. Because multiple types of *O*-mannosyl glycans exist, we propose to designate the *O*-mannosyl glycan structures as cores M1 to M3 (Fig. 4C). Although the sialylated core M1 of DG was originally proposed to be responsible for binding to ligands in the ECM (15), recent glycomics analysis suggests that proteins besides DG are subject to modification of sialylated cores M1 and M2 (16). The fact that LARGE alone could not modify phosphorylated GalNAc- β 3-GlcNAc- β 4-Man- α -MU by using UDP-Xyl and UDP-GlcA as substrate (fig. S13) suggests that CMD causative proteins (FKRP, FKTN, TMEM5, and B3GNT1) besides LARGE are likely to contribute to maturation of the ECM-binding moiety on the phosphorylated core M3 glycan.

References and Notes

1. D. E. Michele *et al.*, *Nature* **418**, 417–421 (2002).
2. R. Barresi, K. P. Campbell, *J. Cell Sci.* **119**, 199–207 (2006).
3. T. Yoshida-Moriguchi *et al.*, *Science* **327**, 88–92 (2010).
4. K. Inamori *et al.*, *Science* **335**, 93–96 (2012).
5. T. Willer *et al.*, *Nat. Genet.* **44**, 575–580 (2012).
6. S. Vuillaumier-Barrot *et al.*, *Am. J. Hum. Genet.* **91**, 1135–1143 (2012).

7. K. Buysse *et al.*, *Hum. Mol. Genet.* **22**, 1746–1754 (2013).
8. M. C. Manzini *et al.*, *Am. J. Hum. Genet.* **91**, 541–547 (2012).
9. E. Stevens *et al.* UK10K Consortium, *Am. J. Hum. Genet.* **92**, 354–365 (2013).
10. L. T. Jae *et al.*, *Science* **340**, 479–483 (2013); 10.1126/science.1233675.
11. H. Many *et al.*, *Proc. Natl. Acad. Sci. U.S.A.* **101**, 500–505 (2004).
12. T. Hiruma *et al.*, *J. Biol. Chem.* **279**, 14087–14095 (2004).
13. Y. Hara *et al.*, *Proc. Natl. Acad. Sci. U.S.A.* **108**, 17426–17431 (2011).
14. G. Manning, D. B. Whyte, R. Martinez, T. Hunter, S. Sudarsanam, *Science* **298**, 1912–1934 (2002).
15. A. Chiba *et al.*, *J. Biol. Chem.* **272**, 2156–2162 (1997).
16. S. H. Stalnak *et al.*, *J. Biol. Chem.* **286**, 21180–21190 (2011).

Acknowledgments: We thank all members of the Campbell laboratory, C. M. Brenner, and C. M. Blaumueller for fruitful discussions; Y. Hara for making an adenovirus vector; H. van Bokhoven for providing patient cells; J. R. Levy for helping imaging studies; H. Nguyen for graphical arts; and the University of Iowa Proteomics Facility and Gene Transfer Vector Core for their services. This work was supported in part by a Paul D. Wellstone Muscular Dystrophy Cooperative Research Center grant (1U54NS053672, K.P.C.), the Muscular Dystrophy Campaign, and the Great Ormond Street Hospital Children Charity (F.M.). K.P.C. is an Investigator of the Howard Hughes Medical Institute. The data are included in the paper and the supplementary materials.

Supplementary Materials

www.sciencemag.org/cgi/content/full/science.1239951/DC1
Materials and Methods
Figs. S1 to S13
Tables S1 and S2
References (17–23)

2 May 2013; accepted 25 July 2013
Published online 8 August 2013;
10.1126/science.1239951

Conformational Motions Regulate Phosphoryl Transfer in Related Protein Tyrosine Phosphatases

Sean K. Whittier,¹ Alvan C. Hengge,² J. Patrick Loria^{1,3*}

Many studies have implicated a role for conformational motions during the catalytic cycle, acting to optimize the binding pocket or facilitate product release, but a more intimate role in the chemical reaction has not been described. We address this by monitoring active-site loop motion in two protein tyrosine phosphatases (PTPs) using nuclear magnetic resonance spectroscopy. The PTPs, YopH and PTP1B, have very different catalytic rates; however, we find in both that the active-site loop closes to its catalytically competent position at rates that mirror the phosphotyrosine cleavage kinetics. This loop contains the catalytic acid, suggesting that loop closure occurs concomitantly with the protonation of the leaving group tyrosine and explains the different kinetics of two otherwise chemically and mechanistically indistinguishable enzymes.

Molecular motions are crucial for the optimal functioning of enzymes. There has been much debate regarding what

role motions play in the enzymatic conversion of substrates to products (1, 2), and recent studies, primarily solution nuclear magnetic resonance (NMR) relaxation experiments, have shown that enzyme motions are critical for optimizing the active site (3–6), enabling effective substrate or cofactor binding (7), and facilitating product dissociation (8). These motions often require collective movement of many amino acids over substantial molecular distances (9) and are

¹Department of Molecular Biophysics and Biochemistry, Yale University, 260 Whitney Avenue, New Haven, CT 06520, USA.

²Department of Chemistry and Biochemistry, Utah State University, 0300 Old Main Hill, Logan, UT 84322, USA. ³Department of Chemistry, Yale University, 225 Prospect Street, New Haven, CT 06520, USA.

*Corresponding author. E-mail: patrick.loria@yale.edu